

Fig. 3 Variation of UT_1/δ and $U_*^2 T_2/\nu$ with Reynolds number.

mean temperature T_2 . A typical trace of the signal is shown in Fig. 1, illustrating the method adopted for identifying the two time scales. For the evaluation of T_1 and T_2 , a sufficient length of the trace was used until consistent average values were obtained. Based on these data, the nondimensional parameters (namely, UT_1/δ , UT_2/δ , $U_*^2 T_1/\nu$, and $U_*^2 T_2/\nu$) were calculated and the results are shown in Figs. 2 and 3. It can be observed that the values of UT_2/δ and $U_*^2 T_1/\nu$ are nearly constant at 1.9 and 40, respectively, irrespective of Reynolds number R_θ , whereas UT_1/δ as well as $U_*^2 T_2/\nu$ vary with R_θ . The value of UT_2/δ obtained in the present investigation is in reasonable agreement with earlier measurements of zero crossings of the fluctuating turbulence signals,⁶ as well as with the results obtained employing autocorrelation and selective filtering techniques.³⁻⁵ Hence, it is justifiable to assume that T_2 in the present measurements represents the period when large eddy-like structures are present in boundary-layer flows.

The independence of $U_*^2 T_1/\nu$ with R_θ presents an entirely different picture, which suggests that the wall shear fluctuations are influenced by some effect different from the large-scale motions. This result seems to have relevance to the streaks and oscillatory motions, observed by Kim et al.¹ very close to the wall in a turbulent boundary layer, that later coagulated into bursts in a quasiperiodic manner. According to them, the period of these visually observed bursts (T_3) follows the relation, $T_3 = 0.001102 U_*^2$, where T_3 is in seconds and U_* is in feet/second. Assuming that their experiments were carried out at a comfortable temperature of 30°C, the kinematic viscosity for water being 1.77/105 m²/s, the value of $U_*^2 T_3/\nu$ would be around 110.0 and independent of R_θ . This value of 110.0 is nearly twice from that of $U_*^2 T_1/\nu$ in the present experiments. However, their independence with R could mean that T_1 and T_3 are governed by the same physical process. The authors speculate that these wall eruptions might undergo pairing as they are lifted away from the wall, hence $T_3 = 2T_1$.

References

- Kim, H. T., Kline, S. J., and Reynolds, W. C., "The Production of Turbulence near a Smooth Wall in a Turbulent Boundary Layer," *Journal of Fluid Mechanics*, Vol. 50, 1971, pp. 133-160.
- Carino, E. R. and Brodkey, R. S., "A Visual Investigation of the Wall Region in Turbulent Flows," *Journal of Fluid Mechanics*, Vol. 37, 1969, pp. 1-30.
- Narahari Rao, K., Narasimha, R., and Badri Narayanan, M. A., "The Bursting Phenomenon in a Turbulent Boundary Layer," *Journal of Fluid Mechanics*, Vol. 48, 1971, pp. 339-352.
- Lauffer, J. and Badri Narayanan, M. A., "Mean Period of the Turbulent Production Mechanism in a Boundary Layer," *Physics of Fluids*, Vol. 14, 1971, pp. 182-183.

⁵Badri Narayanan, M. A. and Marvin, J. G., "On the Period of the Coherent Structure in Boundary Layers at Large Reynolds Numbers," *Proceedings, Coherent Structure of Turbulent Boundary Layers*, Lehigh University, Bethlehem, Pa., 1978, pp. 380-385.

⁶Badri Narayanan, M. A., Rajagopalan, S., and Narasimha, R., "Experiments on the Fine Structure of Turbulence," *Journal of Fluid Mechanics*, Vol. 80, 1977, pp. 237-257 (also Dept. of Aeronautical Engineering, Indian Institute of Science, Bangalore, Rept. 74 FM 15, 1974.)

⁷Lauffer, J., "New Trends in Experimental Turbulence Research," *Annual Review of Fluid Mechanics*, Vol. 17, 1973, pp. 307-326.

⁸Ramaprian, B. R. and Shivaprasad, B. G., "The Instantaneous Structure of Mildly Curved Turbulent Boundary Layers," *Journal of Fluid Mechanics*, Vol. 115, 1982, pp. 39-58.

A New Aerodynamic Integral Equation Based on an Acoustic Formula in the Time Domain

F. Farassat*

NASA Langley Research Center, Hampton, Virginia

Nomenclature

b	$= \lambda M_t + \lambda_l t_l$; $b = b $
b_v	$= b \cdot v$
c	$=$ speed of sound
g	$= \tau - t + r/c$
H	$=$ local mean curvature of the blade surface
h_n	$= \lambda M_n + \lambda_l \cos \theta$
M	$=$ local Mach number vector based on c , $M_n = M \cdot n$, $M_r = M \cdot \hat{r}$
M_p	$=$ projection of the local Mach number vector on the local plane normal to the edges (e.g., trailing edge) of the blade surface, $M_p = M_p $
M_t	$=$ projection of M on the local tangent plane of the blade surface for fixed source time τ , $M_t = M_t = v_t/c$
n, n_i	$=$ unit normal to $f=0$, τ fixed
p'	$=$ acoustic pressure
$p_B(\eta, \tau)$	$\equiv p[y(\eta, \tau), \tau]$ blade surface pressure described in a frame moving with the blades
Q_F, Q_N	$=$ Eqs. (3a) and (3b), respectively
Q_F	$= (M_n - M_t \cdot \Omega)/c + M_t^2 \kappa_t - 2M_n^2 H$
r, r_i	$= x - y, r = x - y $
\hat{r}, \hat{r}_i	$=$ unit radiation vector r/r
\hat{r}_p	$=$ unit vector in the direction of the projection of r on the local plane normal to the edges (e.g., trailing edge) of blade surface, τ fixed
t_l	$=$ projection of the unit radiation vector \hat{r} on the local tangent plane to $f=0$, τ fixed (not unit vector $ t_l = \sin \theta$)
α_n	$= (1 + M_n^2)^{1/2}$
θ	$=$ angle between n and r
κ_l, κ_2	$=$ principal curvatures
κ_b	$=$ normal curvature along b
κ_t	$=$ normal curvature along t
λ	$= (\cos \theta - M_n)/\tilde{\Lambda}^2$
λ_l	$= (\cos \theta + M_n)/\tilde{\Lambda}^2$
Λ	$= (1 + M_n^2 - 2M_n \cos \theta)^{1/2}$
$\tilde{\Lambda}$	$= (\Lambda^2 + \sin^2 \theta)^{1/2}$
Λ_0	$= [M_p^2 \cos^2 \psi + (1 - M_p \cdot \hat{r}_p \sin \psi)^2]^{1/2}$

Received Aug. 10, 1983; revision received Dec. 13, 1983. This paper is declared a work of the U.S. Government and therefore is in the public domain.

*Aeroacoustics Branch, Acoustics and Noise Reduction Division.

- ν, ν_i = unit inward surface vector perpendicular to an edge (e.g., trailing) of the surface $f=0$, τ fixed
 ρ_0 = density of undisturbed medium
 $\sigma, \sigma_i, \sigma_b$ = length parameter on $f=0$ along M_i , t_i , and b , respectively
 σ_{11}, σ_{22} = two components of tensor $(t_i t_i - M_i M_i + t_i M_i + M_i t_i) / \bar{\Lambda}^2$
 ψ = local angle between r and an edge of $f=0$
 Ω, Ω_i = $\mathbf{n} \times \boldsymbol{\omega}$
 $\boldsymbol{\omega}$ = angular velocity

Introduction

A RECENT article by Hanson¹ presents two integral equations for the calculation of aerodynamic loads on advanced propellers. One of these equations [Ref. 1, Eq. (25)] is based on the acceleration potential approach. Hanson's integral equations are obtained from an acoustic formulation in the frequency domain for infinitely thin airfoils. His final results are applicable to propellers moving at uniform forward and angular velocities. Thus, unsteady aerodynamic effects can be analyzed if the mean blade position in space lies on a helicoidal surface generated by such uniform motion of the propeller.

Recently, Long² has derived an integral equation for aerodynamic calculations based on an acoustic formula in the time domain derived by the present author.³ Long has demonstrated the usefulness of this approach by several applications. His main result is valid for bodies moving at subsonic speed. It is the purpose of this Note to present a new aerodynamic integral equation for bodies moving at transonic and supersonic speeds based on a new acoustic formula in the time domain.⁴

Derivation of the Main Result

The present derivation is based principally on Eq. (36) of Ref. 4, which was derived to calculate the noise of the outer portion of the blade traveling at high speed. The acoustic formulation is based on the Ffowcs Williams-Hawkins (FW-H) equation,⁵ retaining only the thickness and loading terms. In the following, the conventional thickness source term, rather than the Isom⁶ one used in Ref. 4, will be utilized. The governing equation for a moving body described by $f=0$ is

$$\square^2 p' = \nabla_4 \cdot [(-pn, \rho_0 cv_n) | \nabla f | \delta(f)] \quad (1)$$

where $\nabla_4 = (\nabla, \partial/c\partial t)$.

The solution of this equation for the loading noise, which involves two surface and three line integrals, is

$$\begin{aligned}
 4\pi p'(x, t) = & \int_{F=0} \frac{1}{r} \left[\frac{1}{\Lambda} \left(pQ_F + \frac{\lambda}{c} \frac{\partial p_B}{\partial \tau} - b \frac{\partial p_B}{\partial \sigma_b} \right) \right]_{\text{ret}} d\Sigma \\
 & + \int_{F=0} \frac{1}{r^2} \left(\frac{pQ_N}{\Lambda} \right)_{\text{ret}} d\Sigma - \int_{\text{TE}} \frac{1}{r} \left[\frac{(pb_v)_u + (pb_v)_l}{\Lambda_0} \right]_{\text{ret}} d\gamma \\
 & - \int_{\text{Shock traces}} \frac{1}{r} \left(\frac{b_v \Delta p}{\Lambda_0} \right)_{\text{ret}} d\gamma - \int_{\text{DEFD}} \frac{1}{r} \left(\frac{b_v p}{\Lambda_0} \right)_{\text{ret}} d\gamma \quad (2)
 \end{aligned}$$

In this equation, $r = |x - y|$ where x and y are the observer and source positions, respectively, and τ the source time. The surface Σ is defined by $[f(y, \tau)]_{\text{ret}} = F(y; x, t) = 0$ and the curve γ is generated by the intersection of the collapsing sphere $g = \tau - t + r/c = 0$ and the edges and shock traces on the blade, see Fig. 1. Other symbols are defined in the Nomenclature. In

addition, we define

$$\begin{aligned}
 Q_F = & \frac{1}{c} \left[\left(2\lambda^2 - \frac{1}{\bar{\Lambda}^2} \right) \dot{M}_n - 2\lambda b \cdot \Omega - \frac{1}{\bar{\Lambda}^2} (t_i - M_i) \cdot \Omega \right. \\
 & \left. + \left(\frac{1}{\bar{\Lambda}^2} + 2\lambda \lambda_i \right) \dot{r} \cdot \Omega \right] + 2b^2 \kappa_b + \sigma_{11} \kappa_1 + \sigma_{22} \kappa_2 - 2Hh_n \quad (3a)
 \end{aligned}$$

$$Q_N = \lambda [2(\cos \theta - M_n) \lambda_i + I] \quad (3b)$$

Note that we have corrected a misprint in Q_F and an error in Q_N in the original reference.⁴ Also the line integral over the trailing edge (TE) is written in a more general form that is valid when the Kutta condition does not hold. The subscripts u and l stand for the upper and lower surfaces, respectively. For thickness noise, in Eq. (2) replace p and p_B by $\rho_0 v_n^2$ in the surface integrals adding Q'_F to the term in parentheses of the first integral. In the line integrals over TE and DEFD, replace pb_v by $\rho_0 c^2 M_n b'_v$ where we have defined $b'_v = (M_n b + M_i) \cdot v$. There are no line integrals over the shock traces.

To derive the aerodynamic result, one must move the observer onto the surface of the blade. However, it can be shown that the second surface integral in Eq. (2) and a similar one for the thickness term are divergent. In fact, it is of the type known as semiconvergent, that is, it can be given a value by regularizing the integral (or taking the principal value in some sense). It is helpful to recognize that there are many ways of regularizing divergent integrals, leading to different analytic expressions for the aerodynamic integral equation, all of which are equivalent.^{2,7} The particular regularization selected must be tailored to numerical calculations. In the present derivation, a regularization of the near-field term of the acoustic formula based on the collapsing sphere approach will be presented. This is done because the collapsing sphere approach is the preferred technique in noise calculations of bodies moving at transonic or supersonic speeds. The process is described as follows. Remove a small hole from the body surface $f=0$ in such a way that the near-field integral is convergent. This is possible because of the semiconvergence property of the integral. Next move the observer to the cap of the hole and evaluate the integral as the observer reaches the

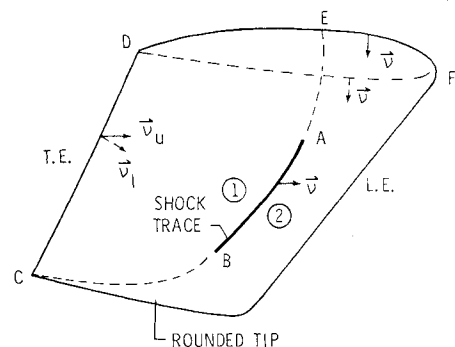


Fig. 1 Geometry of the supersonic portion of the blade.

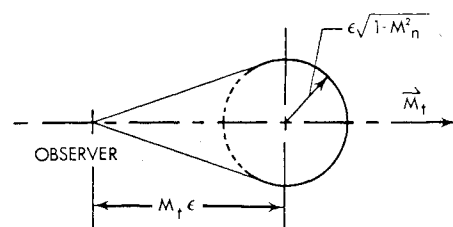


Fig. 2 Shape of the hole used on the body surface to regularize the divergent integral of Eq. (2).

surface of the cap. The shape of the hole cut from the surface in this Note is produced by the collapsing sphere of radius $r < \epsilon$, where $\epsilon > 0$ is a small fixed number. The observer is assumed to reach the surface when $r = 0$. The shape of the hole is shown in Fig. 2 for the observer on the supersonic portion of the blade.

It is easy to show that the near-field term, which is

$$I = \int_{\Gamma} \frac{I}{r^2} \left[\frac{(p + \rho_0 v_n^2) Q_N}{\Lambda} \right] d\Sigma = \int_{\Gamma} \frac{c(p + \rho_0 v_n^2) Q_N}{r^2 \sin \theta} d\Gamma d\tau \quad (4)$$

is now convergent. To see this, note that when the observer reaches the surface at time t , the corresponding collapsing sphere intersects the local tangent plane in a circle (Γ curve) along with $\cos \theta = M_n$ [see Eq. (6a), letting $\delta = 0$]. Since Q_N is proportional to λ and the latter is proportional to $\cos \theta - M_n$, the high-order singularity of Eq. (4) is removed. We now must find the contribution of the cap of the hole, which is of the shape shown in Fig. 2.

The limiting process to calculate the contribution of the cap is as follows. Take $\delta > 0$, fix ϵ , and set the observer at a vertical distance δ above the desired point on the surface at time t . Evaluate the integral in Eq. (4) and then let δ approach zero. Finally, let ϵ approach zero also. We assume $c(t - \tau) < \epsilon$ in the collapsing process of $g = 0$. Figure 3 shows the geometry of the collapsing sphere process at two times. The two planes are the local tangent planes. By expanding $q = p + \rho_0 v_n^2$ in a Taylor series in the vicinity of the observer position, we note that we must study the contribution of the cap to the integral

$$I = q_0 \int_{\Gamma} \frac{c Q_N}{r^2 \sin \theta} d\Gamma d\tau \quad (5)$$

where q_0 is the value of q at the observer position. In the integral above, the time integration is over $c\tilde{\tau} < \epsilon$, where $\tilde{\tau} = t - \tau$. The above integral can be evaluated analytically as follows.

Referring to Fig. 3, note that

$$\cos \theta = M_n + \frac{\delta}{c\tilde{\tau}} \quad (6a)$$

$$R = r \sin \theta \quad (6b)$$

$$\int_{t-\frac{\epsilon}{c}}^{t-\frac{\epsilon}{c}} \int_{r=ct}^{\epsilon} \frac{cd\Gamma d\tau}{r^2 \sin \theta} = -2\pi \int_{\tau_1}^{\epsilon} \frac{cd\tilde{\tau}}{r} \quad (6c)$$

where τ_1 is the value of $\tilde{\tau}$ when the collapsing sphere leaves the body. From Eqs. (5) and (6c), the following is obtained

$$\begin{aligned} \frac{I}{q_0} &= -2\pi \int_{\tau_1}^{\epsilon} \frac{\lambda}{r} cd\tilde{\tau} - 4\pi \int_{\tau_1}^{\epsilon} \frac{(\cos \theta - M_n) \lambda \lambda_I}{r} cd\tilde{\tau} \\ &\equiv -2\pi I_1 - 4\pi I_2 \end{aligned} \quad (7)$$

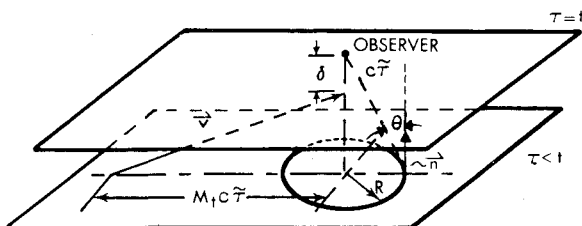


Fig. 3 Geometry of the intersection of the collapsing sphere with the local tangent plane for the evaluation of Eq. (5).

An easy way to integrate I_1 and I_2 is to introduce the new variable $z = \cos \theta$ and use Eq. (6a). It is found that

$$I_1 = - \int \frac{dz}{2\alpha_n^2 - (z + M_n)^2} \quad (8)$$

$$\begin{aligned} I_2 &= \int \frac{dz}{2\alpha_n^2 - (z + M_n)^2} + M_n \int \frac{2(z + M_n) dz}{[2\alpha_n^2 - (z + M_n)^2]^2} \\ &\quad - 2\alpha_n^2 \int \frac{dz}{[2\alpha_n^2 - (z + M_n)^2]^2} \end{aligned} \quad (9)$$

The limits of all these integrals are from $M_n + \delta/\epsilon$ to 1. The integrals in Eqs. (8) and (9) can now be evaluated to yield

$$\frac{I}{q_0} = -2\pi \left[\frac{M_n - z}{2\alpha_n^2 - (z + M_n)^2} \right]_{M_n + \frac{\delta}{\epsilon}}^1 + \frac{\delta}{\epsilon} \quad (10)$$

After substituting the limits and letting $\delta \rightarrow 0$, we obtain

$$I = \frac{2\pi q_0}{1 - M_n} \quad (11)$$

Our main result is obtained by noting that p' on the left of Eq. (2) is in fact p . We now drop the subscript of q_0 and use $p + \rho_0 v_n^2$ instead. Using Eq. (11), Eq. (2) can now be written as

$$4\pi \left[I - \frac{I}{2(1 - M_n)} \right] p = \frac{2\pi \rho_0 v_n^2}{1 - M_n} + I_e \quad (12)$$

Here I_e denotes all the acoustic integrals with the surface integrals evaluated on $f = 0$ with a hole of the shape shown in Fig. 2. Equation (12) is the aerodynamic integral equation in time domain and is the main result of this Note.

Conclusion

Equation (12) is a singular integral equation that must be solved to find the unknown surface pressure p . It was derived for application to advanced high-speed propellers where the use of thin blade sections allows linearization of the aerodynamic problem. There is little hope of obtaining a closed-form analytic solution of Eq. (12) for such propellers due to the complexity of modern designs. However, numerical techniques such as the Galerkin or collocation methods are available.

It should be noted that the present integral equation does not have some of the restrictions imposed in the derivation of Hanson's equations.¹ These restrictions are an infinitely thin airfoil, the uniform propeller-like motion of blades, and the approximation of source positions on a helicoidal surface. The arbitrary motion of the blades in the present formulation will allow the study of nonuniform in-flow to the propeller. It is also noted that no complicated infinite series of special functions with questionable convergence properties appear in the present formulation. The experience of Long in solving the subsonic integral equation^{2,3} indicates that the matrices involved in the inversion process are well behaved. This is another important advantage of using integral equations in the time domain as compared to those derived in the frequency domain.

It is seen that, for a blade with a blunt leading edge (LE) and moving at supersonic speed, there is a singularity in the integral equation near the LE where $M_n = 1$. However, the assumption of small perturbations breaks down near the blunt LE, making the integral equation invalid. The present generation of blades uses sections with very small LE radius that can be assumed sharp. However, another line integral over the leading edge similar to that over the trailing edge will appear in the acoustic formulation.

References

- ¹Hanson, D. B., "Compressible Helicoidal Surface Theory for Propeller Aerodynamics and Noise," *AIAA Journal*, Vol. 21, June 1983, pp. 881-889.
- ²Long, L. N., "The Compressible Aerodynamics of Rotating Blades Using an Acoustic Formulation," Ph.D. Dissertation, School of Engineering and Applied Science, George Washington University, Washington, D.C., April 1983.
- ³Long, L. N., "The Aerodynamics of Propellers and Rotors Using an Acoustic Formulation in the Time Domain," AIAA Paper 83-1821, 1983.
- ⁴Farassat, F., "The Prediction of the Noise of Supersonic Propellers in Time Domain—New Theoretical Results," AIAA Paper 83-0743, April 1983.
- ⁵Ffowes Williams, J. E. and Hawkings, D. L., "Sound Generated by Turbulence and Surfaces in Arbitrary Motion," *Philosophical Transactions of the Royal Society of London*, Vol. A264, 1969, pp. 321-342.
- ⁶Isom, M. P., "The Theory of Sound Radiated by a Hovering Transonic Helicopter Blade," Polytechnic Institute of New York, Rept. Poly-AE/AM 75-4, 1975.
- ⁷Farassat, F., "Advanced Theoretical Treatment of Propeller Noise," *Propeller Performance and Noise*, von Kármán Institute for Fluid Dynamics, Lecture Series 1982-08, 1982.

Steady-State Response of Vibrating Systems to Periodic Pulse Excitation

R. B. Bhat*

Concordia University, Montreal, Quebec, Canada

Introduction

MACHINES and structures are often subjected to periodic pulse excitations. Examples include punch presses, rolling mills, gear teeth, and internal combustion engines. Two common methods to obtain the steady-state response of such a system are:

- 1) The Fourier series method, in which the periodic pulse excitation is expanded in a Fourier series and the system response to each term in the series is summed.
- 2) The Laplace transform method.

Both methods involve summation of series. In this Note, a simple closed-form expression is obtained for the steady-state response of a system, using the convolution integral along with the unit impulse response.¹

Analysis

The equation of motion of a simple vibrating system with mass m , stiffness k , and damping coefficient c can be written as

$$\ddot{x} + 2\zeta\omega_n\dot{x} + \omega_n^2x = F(t)/m$$

$$\begin{aligned} F(t) &= F_0 \quad nT < t < nT + t_f \\ &= 0 \quad nT + t_f < t < (n+1)T \quad n=0,1,2,\dots \\ x &= \dot{x} = 0 \text{ for } t < 0 \end{aligned} \quad (1)$$

where $\omega_n = (k/m)^{1/2}$ is the system natural frequency, $\zeta = c/2m\omega_n$ the damping ratio, T the period of the excitation

function, and t_f the duration of the pulse within a period. The periodic pulse excitation $F(t)$ is shown in Fig. 1.

Assuming that steady-state conditions are obtained after sufficiently large $n=N$, the system response will satisfy the following conditions:

$$\begin{aligned} x(NT) &= x[(N+1)T] = A \\ \dot{x}(NT) &= \dot{x}[(N+1)T] = B \end{aligned} \quad (2)$$

where A and B are to be determined.

The system response during $NT < t < (N+1)T$ may be written as

$$\begin{aligned} x(\xi) &= \exp(-\zeta\omega_n\xi) \left[A \cos\omega_d\xi + \left(\frac{B + \zeta\omega_n A}{\omega_d} \right) \sin\omega_d\xi \right] \\ &+ \int_0^\xi h(\xi-\tau)F(\tau)d\tau \end{aligned} \quad (3)$$

where $\xi = t - NT$ and $h(t)$ is unit impulse response of the system. Substituting for $h(t)$ (Ref. 1) and $F(t)$ in Eq. (3), the following response is obtained:

$$\begin{aligned} x(\xi) &= \exp(-\zeta\omega_n\xi) \left[A \cos\omega_d\xi + \left(\frac{B + \zeta\omega_n A}{\omega_d} \right) \sin\omega_d\xi \right] \\ &+ \frac{1}{m\omega_d\omega_n^2} \{ \omega_d - \exp(-\zeta\omega_n\xi) [\zeta\omega_n \sin\omega_d\xi + \omega_d \cos\omega_d\xi] \} \\ &\quad 0 < \xi < t_f \\ &= \exp(-\zeta\omega_n\xi) \left[A \cos\omega_d\xi + \left(\frac{B + \zeta\omega_n A}{\omega_d} \right) \sin\omega_d\xi \right] \\ &+ \frac{1}{m\omega_d\omega_n^2} \{ \exp(-\zeta\omega_n\xi^*) [\zeta\omega_n \sin\omega_d\xi^* + \omega_d \cos\omega_d\xi^*] \\ &\quad - \exp(-\zeta\omega_n\xi) [\zeta\omega_n \sin\omega_d\xi + \omega_d \cos\omega_d\xi] \} \quad t_f < \xi < T \end{aligned} \quad (4)$$

where $\xi^* = \xi - t_f$. Utilizing the conditions of Eq. (2) in Eq. (4), it is possible to obtain equations of the form:

$$a_{11}A + a_{12}B = a_{13} \quad a_{21}A + a_{22}B = a_{23} \quad (5)$$

The constants A and B are obtained by solving Eq. (5) as

$$\begin{aligned} A &= (a_{13}a_{22} - a_{23}a_{12}) / (a_{11}a_{22} - a_{21}a_{12}) \\ B &= (a_{11}a_{23} - a_{21}a_{13}) / (a_{11}a_{22} - a_{21}a_{12}) \end{aligned} \quad (6)$$

The steady-state response is obtained by using these values of A and B in Eq. (4).

The response of the system obtained by summing the responses of the system to each term in the Fourier series

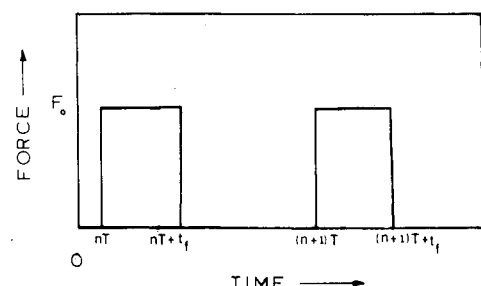


Fig. 1 Periodic pulse excitation.